Acta Cryst E CRYSTALLOGRAPHIC COMMUNICATIONS

ISSN 2056-9890

Crystal structure and Hirshfeld surface analysis of 10-([2,3′-bithiophen]-5′-yl)-5,5-difluoro-5*H*-4λ^4,5λ^4-dipyrrolo[1,2-*c*:2′,1′-*f*][1,3,2]diazaborinine

Darya K. Polyanskaya,[a] Zlata A. Polianskaia,[a] Victor N. Khrustalev,[a,b] Mehmet Akkurt,[c] Gizachew Mulugeta Manahelohe,[d]* Khudayar I. Hasanov[e] and Narmina A. Guliyeva[f]

[a]RUDN University, 6 Miklukho-Maklaya St., Moscow 117198, Russian Federation, [b]Zelinsky Institute of Organic Chemistry of RAS, Leninsky Prospect 47, Moscow 119991, Russian Federation, [c]Department of Physics, Faculty of Sciences, Erciyes University, 38039 Kayseri, Türkiye, [d]Department of Chemistry, University of Gondar, PO Box 196, Gondar, Ethiopia, [e]Azerbaijan Medical University, Scientific Research Centre (SRC), A. Kasumzade St. 14, AZ 1022, Baku, Azerbaijan, and [f]Department of Chemical Engineering, Baku Engineering University, Hasan Aliyev str. 120, Khirdalan, Absheron AZ0101, Azerbaijan. *Correspondence e-mail: Gizachew.Mulugeta@uog.edu.et

Received 28 May 2026
Accepted 21 June 2026

Edited by C. Schulzke, Universität Greifswald, Germany

Keywords: crystal structure; thiophene; S-heterocycle; disorder; Hirshfeld surface analysis.

CCDC reference: 2563746

Supporting information: this article has supporting information at journals.iucr.org/e

In the title compound, $C_{17}H_{11}BF_2N_2S_2$, the molecular conformation is consolidated by an intramolecular C—H···S interaction forming an *S*(6) ring. In the crystal, molecules are linked by C—H···F interactions, forming a three-dimensional network. The terminal thiophene ring is disordered in a 0.659 (3):0.341 (3) ratio around the C—C bond that connects the thiophene rings, with a rotation of approximately 180° around the ring. According to a Hirshfeld surface analysis, H···H (34.8%), C···H/H···C (22.1%) and F···H/H···F (18.6%) interactions are the main contributors to the crystal packing.

1. Chemical context

BODIPY, 4,4-difluoro-4-bora-3a,4a-diaza-*s*-indacene, and its derivatives are well known for their properties as fluorophores. First synthesized in 1968, whereas the core scaffold was isolated and described only in 2009, these compounds represent a prominent class of functional compounds with favorable photophysical properties, including a large molar absorption coefficient, narrow absorption and emission bands, high fluorescence quantum yield, and excellent photochemical stability (Treibs & Kreuzer, 1968; Schmitt *et al.*, 2009; Yadav & Misra, 2023). Owing to these characteristics, they have found widespread applications as fluorescent probes, in cell imaging, as organic light-emitting diodes (OLEDs), dye-sensitized solar cells (DSCs) and in phototherapy (Gai *et al.*, 2023; Gawale *et al.*, 2024; Mao *et al.*, 2023). In particular, BODIPYs have been shown to be promising photosensitizers for photodynamic therapy (PDT), despite certain drawbacks such as absorption at wavelengths below 600 nm, hydrophobicity, and poor tissue penetration (Zhang *et al.*, 2021). The structural versatility of BODIPYs, including modifications at specific positions of the core, enables fine-tuning of their chemical and photophysical properties (*e.g.*, singlet-oxygen generation, emission wavelength, and fluorescence efficiency), thereby enhancing their photodynamic efficacy, biocompatibility, and overall role in imaging and therapeutic applications in PDT (Prieto-Montero *et al.*, 2020; Malacarne *et al.*, 2022). Thus, the photophysical behavior of BODIPY may be governed by the substituent at the *meso*-position, yet replacing the typical six-membered aryl ring with five-membered heterocycles (*e.g.*, furan, thiophene, pyrrole, selenophene) has received limited attention. For

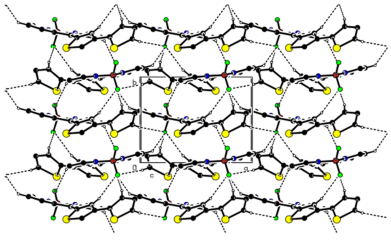

OPEN ACCESS
Published under a CC BY 4.0 licence

example, the insertion of a thiophene ring into this position, followed by modification with a nitrogenous base and the creation of a nucleotide based on it, makes it possible to effectively use the resulting BODIPY scaffold as a fluorescent DNA probe to study bacterial metabolism (Šoltysová *et al.*, 2025). Therefore, studying the introduction of various heterocycles, especially thiophene derivatives, into the *meso*-position remains relevant. Herein, we report the synthesis of a BODIPY derivative functionalized with a thiophene ring at the *meso*-position to investigate its influence on the structural, electronic, and photophysical properties of the resultant fluorophore. Previously, we described a two-stage method for obtaining BODIPY-type structures, where various heterocyclic aldehydes were utilized as starting compounds (Sadikhova *et al.*, 2024; Polianskaia *et al.*, 2026). This strategy was also applied in this study: [2,3′-bithiophene]-5′-carbaldehyde was taken as the starting molecule and introduced into a condensation reaction with pyrrole under acid catalysis in inert atmosphere. The resulting intermediate dipyrrolmethane **1** was then oxidized with DDQ in CH_2Cl_2 (30 min), followed by neutralization with DIPEA and subsequent treatment with $BF_3{\cdot}OEt_2$, providing the corresponding BODIPY complex. The target *meso*-thienyl-substituted BODIPY **2** was isolated in 58% yield after silica gel column chromatography.

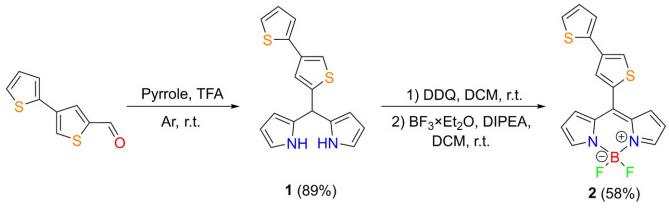

2. Structural commentary

The mean plane of the twelve-membered ring system (C1–C9/N1/B1/N2 with an r.m.s. deviation of fitted atoms of 0.0819 Å) makes a dihedral angle of 37.3 (1)°, with the thiophene ring (S1/C10–C13), while the angles subtended the major and minor components (S2/C14–C17 and S2′/C14/C15′–C17′) of the terminal thiophene ring and the twelve-membered ring system are 50.9 (3) and 48.8 (6)°, respectively (Fig. 1). The molecular conformation is consolidated by an intramolecular C7—H7···S1 hydrogen bond, forming an *S*(6) motif (Fig. 1, Table 1; Bernstein *et al.*, 1995). The BODIPY torsion angles F1—B1—N1—C4 and F2—B1—N2—C6 are −103.5 (2) and −135.5 (2)°, respectively. All geometric parameters are normal and consistent with those of related compounds discussed in the *Database survey*.

3. Supramolecular features and Hirshfeld surface analysis

In the crystal, molecules are linked by C—H···F interactions, forming a three-dimensional framework (Table 1). A detailed overview of the C—H···F interactions within the unit cell is given in Fig. 2. Crystal packing views along the *a* and *c* axes are shown in Figs. 3 and 4, respectively. C—H···π and π-π interactions are not observed.

Table 1
Hydrogen-bond geometry (Å, °).

D—H···*A*	*D*—H	H···*A*	*D*···*A*	*D*—H···*A*
C3—H3···F2^{i}	0.95	2.55	3.362 (2)	144
C7—H7···S1	0.95	2.68	3.1895 (19)	114
C8—H8···F1^{ii}	0.95	2.43	3.229 (2)	142
C11—H11···F1^{iii}	0.95	2.54	3.4360 (19)	156
C15—H15···F1^{iii}	0.95	2.49	3.426 (13)	168
C17—H17···F1^{iv}	0.95	2.38	3.255 (11)	153

Symmetry codes: (i) $-x+1, y-\frac{1}{2}, -z+1$; (ii) $-x, y+\frac{1}{2}, -z+1$; (iii) $-x+1, y+\frac{1}{2}, -z+1$; (iv) $x+1, y, z+1$.

The Hirshfeld surface and associated two-dimensional fingerprint plots for the title compound were calculated employing established procedures in *CrystalExplorer17.5* (Spackman *et al.*, 2021) to determine the influence of weak intermolecular interactions on the molecular packing. The Hirshfeld surfaces mapped over d_{norm} using a fixed colour scale of −0.24 (red) to 1.22 (blue) a.u. are shown in Fig. 5. The few red spots indicate intermolecular contacts involved in interactions (Tables 1 and 2).

Fig. 6 shows the full two-dimensional fingerprint plot and those delineated into H···H (34.8%), C···H/H···C (22.1%) and F···H/H···F (18.6%) contacts. The most important interaction is H···H, contributing 34.8% to the overall crystal

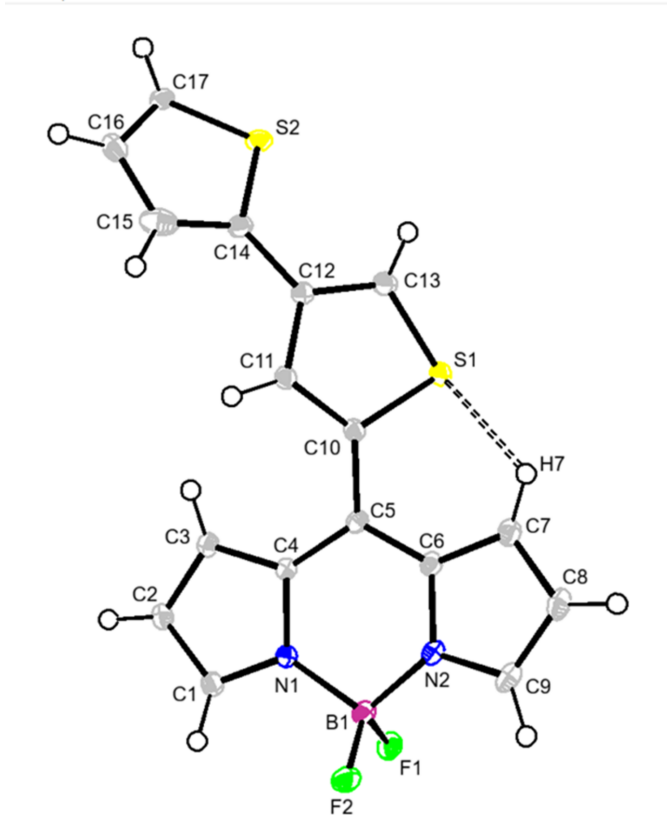

Figure 1
Molecular structure of **2** showing the atomic labelling. Displacement ellipsoids are drawn at the 50% probability level. The intramolecular hydrogen bond is shown as a dashed line.

Table 2
Summary of short interatomic contacts (Å).

Contact	Distance	Symmetry operation
H7···H16A^a	2.57	$1-x, \frac{1}{2}+y, 2-z$
F1···H15^a	2.49	$1-x, -\frac{1}{2}+y, 1-z$
S2^a···H1	3.18	$x, y, 1+z$
F1···*H17	2.38	$-1+x, y, -1+z$
F1···H8	2.43	$-x, -\frac{1}{2}+y, 1-z$
H2···H9	2.56	$1+x, y, z$

Note: (*a*) Atom of the minor occupancy disorder component.

packing, which is reflected in Fig. 6*b* as widely scattered points of high density due to the large hydrogen content of the molecule, with small split tips at $d_e \simeq d_i = 1.25$ Å. The pair of characteristic wings in the fingerprint plot arising from C···H/H···C contacts, Fig. 7*c*, has a 22.1% contribution to the Hirshfeld surface with the tips at $d_e + d_i = 2.70$ Å. The F···H/H···F interactions have a 18.6% contribution to the Hirshfeld surface with a pair of sharp spikes characteristic of quite strong interactions and $d_e + d_i \simeq 2.25$ Å (Fig. 6*d*). Other contacts with smaller contributions to the Hirshfeld surface have a less significant effect on the crystal packing: S···H/H···S (7.1%), C···C (6.9%), S···C/C···S (3.5%), N···H/

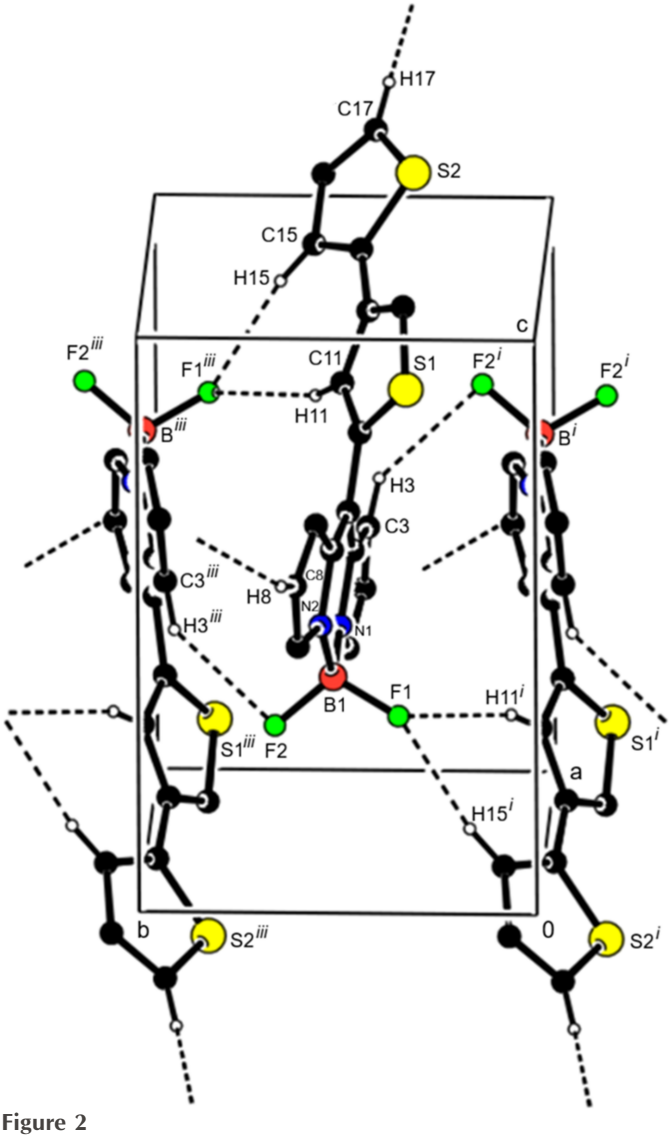

Figure 2
A general view of the C—H···F interactions (dashed lines) in the unit cell. For symmetry codes, see Table 1..

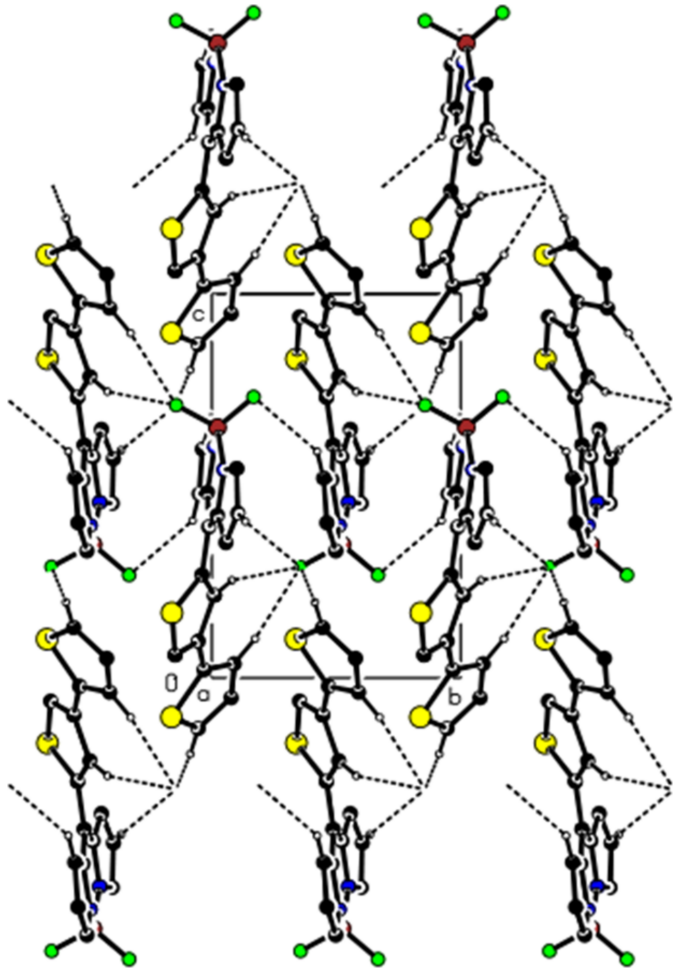

Figure 3
Crystal packing viewed along the *a* axis showing the C—H···F interactions (dashed lines). H atoms not involved in hydrogen bonding are omitted.

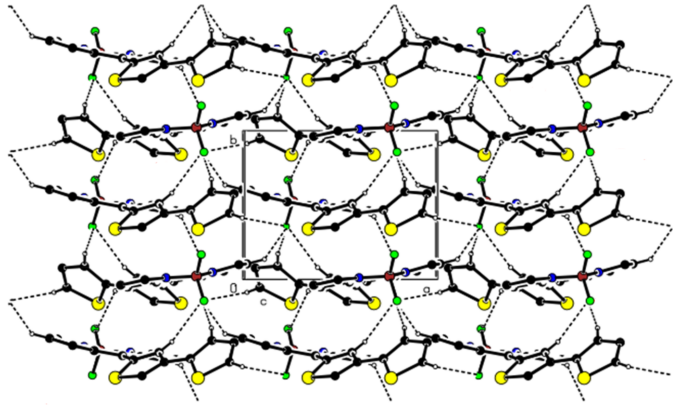

Figure 4
Crystal packing viewed along the *c* axis.

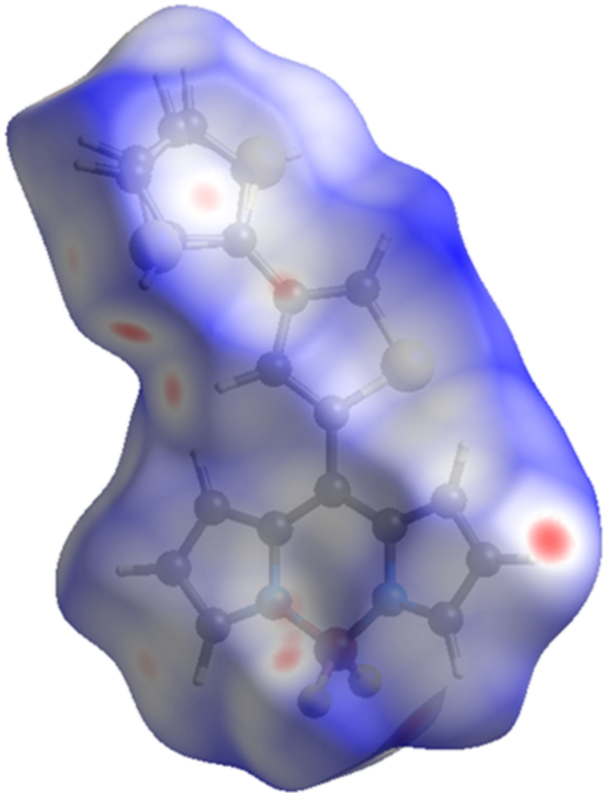

Figure 5
Three-dimensional Hirshfeld surface mapped over d_{norm}.

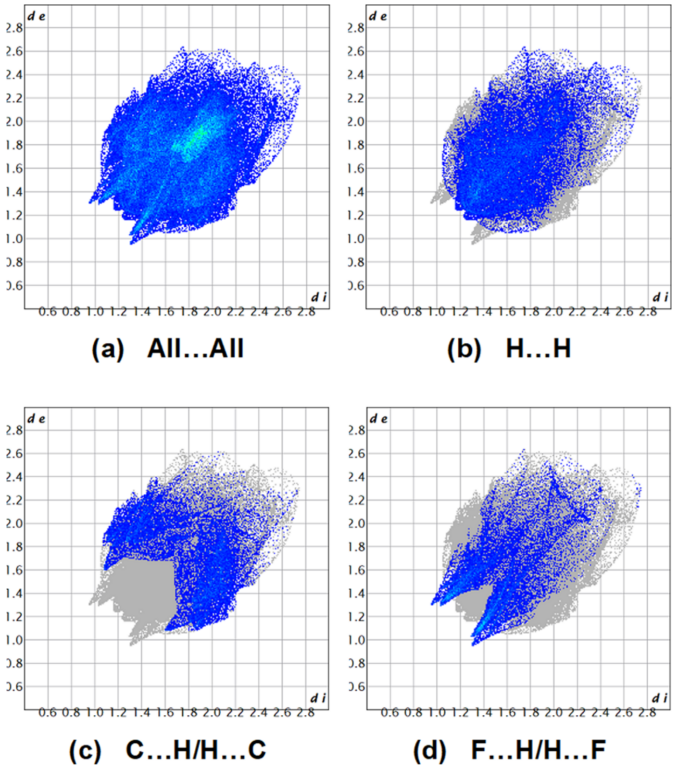

Figure 6
The two-dimensional fingerprint plots showing (*a*) all interactions, and those delineated into (*b*) H···H, (*c*) C···H/H···C and (*d*) F···H/H···F interactions. The d_i and d_e values are the closest internal and external distances (in Å) from given points on the Hirshfeld surface.

H···N (3.3%), F···C/C···F (2.3%), N···C/C···N (0.9%), S···S (0.3%) and F···S/S···F (0.2%).

4. Database survey

A search of the Cambridge Structural Database (CSD, version 6.00, updated April 2025; Groom *et al.*, 2016) for a thiophene-substituted BODIPY revealed five compounds: CSD refcodes DICJOP (Choi *et al.*, 2007), IQOTAM (Ordóñez-Hernández *et al.*, 2021), ROHXEV (Farfán–Paredes *et al.*, 2023), XAHZEO (Xochitiotzi-Flores *et al.*, 2016), and ZEQKEP (Martínez-Bourget *et al.*, 2022); when substitutions on pyrrole were allowed, thirty-four compounds were found (Fig. 7).

DICJOP crystallizes in the orthorhombic $P2_12_12_1$ space group. IQOTAM and ZEQKEP crystallize in the monoclinic space group $P2_1$, while ROHXEV and XAHZEO crystallize in the triclinic $P\overline{1}$ space group.

In DICJOP, C—H···F interactions link molecules to form layers parallel to the *ac* plane (010) with an $R_4^4(26)$ motif protruding along the crystallographic *c* axis and an $R^2{}_2(14)$

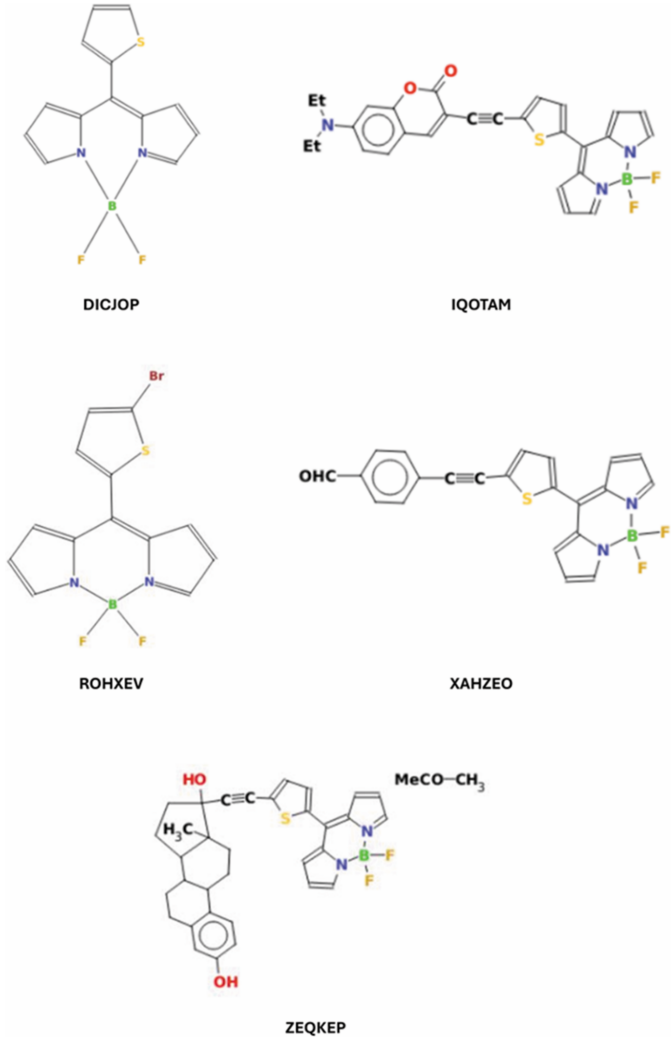

Figure 7
Chemical formulae of compounds DICJOP, IQOTAM, ROHXEV, XAHZEO and ZEQKEP.

motif expanding the layer into the *a* direction. In IQOTAM, there are two independent molecules in the asymmetric unit, which are inversion conformers. They form an extensive three-dimensional network with C—H···F plus C—H···O, C—H···S, C—H···. and π–π interactions. In ROHXEV, the molecules are linked along the *a*-axis direction by C—H···F interactions, forming *C*(8) zigzag chains. These chains are extended into ribbons by bidirectional C—H···F hydrogen bonds forming $R^2_2(10)$ motifs. The chains are linked along the *b*-axis direction by what may be considered weak C—H···π interactions, forming layers parallel to the *ab* plane. In XAHZEO, a bidirectional C—H···F hydrogen-bonding interaction of one fluorine with one adjacent molecule forms an $R^2_2(10)$ ring motif. The second F atom of the BODIPY moiety forms the same hydrogen-bonding motif to the next molecule in the *a*-axis direction. The interactions therefore result in broad ribbons extending along the *a*-axis direction. The ribbons are linked by C—H···O bonds involving an aldehyde function to form layers in the (012) plane. In ZEQKEP, C—H···F interactions form chains along the *ac* diagonal. C—H···O bonds running parallel to the crystallographic *b* axis link the ribbons into zigzag layers somewhat coplanar with the (401) plane.

In conclusion, the observation of C—H···F interactions in all of these structures suggests that this interaction may be generally important in molecular packaging regulation, in particular, for BODIPY derivatives.

5. Synthesis and crystallization

The BODIPY synthesis procedure was reported previously (Sadikhova *et al.*, 2024; Polianskaia *et al.*, 2026). The starting [2,3′-bithiophene]-5′-carbaldehyde (0.45 g, 2.00 mmol) and pyrrole (3.89 g, 58.00 mmol) were placed into a two-neck flask. The reaction mixture was purged with argon for 10 min. Trifluoroacetic acid (TFA, 26.0 mg, 0.20 mmol) was added dropwise to the reaction under stirring at r.t. After that, the reaction mixture was stirred for an hour under argon. Then Et_3N (50 µL) was added to pH ∼7. The reaction mixture was poured into water (50 mL) and extracted with ethyl acetate (3 × 10 mL). The target product was purified by column chromatography (eluent: heptane–ethyl acetate 10:1, TLC: heptane/ethyl acetate 4:1); greyish green powdery crystals, yield 89%, 550 mg (1.77 mmol). ^{1}H NMR (700.2 MHz, $CDCl_3$) (*J*, Hz): δ 8.06 (*br.s*, 2H, NH), 7.27 (*d*, *J* = 1.4 Hz, 1 H, H-2′ Thien), 7.19 (*dd*, *J* = 5.0, 0.9 Hz, 1 H, H-5 Thien), 7.14 (*dd*, *J* = 3.6, 0.9 Hz, 1 H, H-3 Thien), 7.13 (*br.s*, 1 H, H-4′ Thien), 7.02 (*dd*, *J* = 5.0, 3.6 Hz, 1 H, H-4 Thien), 6.75–6.73 (*m*, 2 H, H-5,5′ Pyr), 6.19 (*m*, 2 H, H-4,4′ Pyr), 6.10 (*br.s*, 2 H, H-3,3′ Pyr), 5.75 (*s*, 1 H, CH). ^{13}C NMR (176.1 MHz, $CDCl_3$): δ 146.8, 139.1, 135.2, 131.5 (2 C), 127.6, 124.6, 123.8, 123.1, 118.7, 117.6 (2 C), 108.6 (2 C), 107.2 (2 C), 39.3. Dipyrrolmethane **1** (542 mg, 1.7 mmol) was dissolved in dry dichloromethane (DCM, 30 ml), after 2,3-dichloro-5,6-dicyanobenzoquinone (DDQ, 1.21 g, 5.3 mmol) was added; the reaction mixture was stirred for 30 min (TLC control), poured into water (80 mL) and extracted with DCM (3 × 30 mL). The organic layer was dried with anhydrous Na_2SO_4, concentrated *in vacuo* and the residue was dissolved in dry DCM (20 ml) without further purification. Boron trifluoride etherate (4.5 ml, 34.9 mmol) and an equal volume of diisopropylethylamine (DIPEA, 4.5 ml) were added. The solution was stirred under room temperature for 1 h (TLC control) and then poured into water (80 mL), extracted with DCM (3 × 30 mL) and washed with saturated Na_2CO_3 (3 × 30 mL). The organic layer was dried with anhydrous Na_2SO_4, the target product **2** was purified by column chromatography (eluent: ethyl acetate/hexane 1:10); dark-red crystals, yield 58%, 330 mg (0.92 mmol), m.p. 431–432 K. Single crystals of the title compound were grown using the mixed solvents ethyl acetate–hexane at 281 K. ^{1}H NMR (700.2 MHz, $CDCl_3$) (*J*, Hz): δ 7.96 (*s*, 2 H, H-5,5′ Pyr), 7.73 (*dd*, *J* = 7.6, 1.4 Hz, 2 H, H-4,4′ Pyr), 7.34–7.28 (*m*, 4 H, H-2′,3,4′,5 Thien), 7.10 (*dd*, *J* = 5.2, 3.6 Hz, 1 H, H-4 Thien), 6.61 (*m*, 2 H, H-3,3′ Pyr). ^{13}C NMR (176.1 MHz, $CDCl_3$): δ 144.2 (2 C), 138.8, 137.5, 136.8, 135.2, 134.2, 131.4 (2 C), 131.2, 128.0, 125.0 (2 C), 124.9, 124.2, 118.7 (2 C). ^{19}F NMR (658.8 MHz, $CDCl_3$): δ −144.8–−145.5 (*m*, 2 F). MS (ESI) *m*/*z*: $[M]^+$ 356.

Table 3
Experimental details.

Crystal data	
Chemical formula	$C_{17}H_{11}BF_2N_2S_2$
M_r	356.21
Crystal system, space group	Monoclinic, $P2_1$
Temperature (K)	100
a, *b*, *c* (Å)	9.4693 (2), 7.2412 (1), 11.2392 (2)
β (°)	95.512 (1)
V (Å^3)	767.10 (2)
Z	2
Radiation type	Mo *K*α
μ (mm^{-1})	0.37
Crystal size (mm)	0.20 × 0.12 × 0.10
Data collection	
Diffractometer	Bruker D8 QUEST PHOTON-III area detector
Absorption correction	Multi-scan (*SADABS*; Krause *et al.*, 2015)
T_{min}, T_{max}	0.674, 0.746
No. of measured, independent and observed [$I > 2\sigma(I)$] reflections	24975, 5559, 5142
R_{int}	0.041
(sin $\theta/\lambda)_{max}$ (Å^{-1})	0.758
Refinement	
$R[F^2 > 2\sigma(F^2)]$, $wR(F^2)$, *S*	0.030, 0.072, 1.03
No. of reflections	5559
No. of parameters	255
No. of restraints	147
H-atom treatment	H-atom parameters constrained
$\Delta\rho_{max}$, $\Delta\rho_{min}$ (e Å^{-3})	0.35, −0.22
Absolute structure	Refined as an inversion twin
Absolute structure parameter	0.29 (6)

Computer programs: *APEX3* (Bruker, 2013), *SAINT* (Bruker, 2018), *SHELXS97* (Sheldrick, 2008), *SHELXL2014* (Sheldrick, 2015), *ORTEP-3 for Windows* (Farrugia, 2012) and *PLATON* (Spek, 2020).

6. Refinement

Crystal data, data collection and structure refinement details are summarized in Table 3. All C-bound hydrogen atoms were positioned geometrically (C—H = 0.95 Å) and refined using a

riding model, with $U_{iso}(H) = 1.2\ U_{eq}(C)$. The terminal thiophene ring (S2/C14–C17) is disordered by a 180° rotation over two orientations around the C12—C14 bond in a 0.659 (3):0.341 (3) ratio. The geometries of the disordered components were restrained to be similar (SAME in *SHELXL*). The rigid bond and similar displacement parameter restraints (DELU and SIMU, respectively) were applied for the atoms involved. One outlier reflection (001), affected by the incident beam-stop, was omitted in the last cycles of the refinement.

Acknowledgements

The authors' contributions are as follows; conceptualization AVG, MA and GMM; synthesis, DKP and ZAP; X-ray analysis VNK; founding KAA; writing (review and editing of the manuscript) KAA and MA; supervision AVG, MA and GMM.

Funding information

This publication was supported by the RUDN University (project within the framework of the competition for grant funding of young scientists 'Joint start: Making science together') as well as by the Azerbaijan Medical University and Baku Engineering University.

References

Bernstein, J., Davis, R. E., Shimoni, L. & Chang, N.-L. (1995). *Angew. Chem. Int. Ed. Engl.* **34**, 1555–1573.
Bruker (2013). *APEX3*. Bruker AXS Inc., Madison, Wisconsin, USA.
Bruker (2018). *SAINT*. Bruker AXS Inc., Madison, Wisconsin, USA.
Choi, S. H., Kim, K., Lee, J., Do, Y. & Churchill, D. G. (2007). *J. Chem. Crystallogr.* **37**, 315–331.
Farfán–Paredes, M., Labra–Vázquez, P., González–Antonio, O., Martínez–Bourget, D., Guzmán–Cedillo, C., Galindo–Hernández, A., Romero, M., Santillan, R. & Farfán, N. (2023). *Chem. A Eur. J.* **29**, e202302847.
Farrugia, L. J. (2012). *J. Appl. Cryst.* **45**, 849–854.
Gai, L., Liu, Y., Zhou, Z., Lu, H. & Guo, Z. (2023). *Coord. Chem. Rev.* **481**, 215041.
Gawale, Y., Palanisamy, P., Lee, H. S., Chandra, A., Kim, H. U., Ansari, R., Chae, M. Y. & Kwon, J. H. (2024). *Appl. Mater. Interfaces* **16**, 22274–22281.
Groom, C. R., Bruno, I. J., Lightfoot, M. P. & Ward, S. C. (2016). *Acta Cryst.* B**72**, 171–179.
Krause, L., Herbst-Irmer, R., Sheldrick, G. M. & Stalke, D. (2015). *J. Appl. Cryst.* **48**, 3–10.
Malacarne, M. C., Gariboldi, M. B. & Caruso, E. (2022). *Int. J. Mol. Sci.* **23**, 10198.
Mao, Z., Kim, J. H., Lee, J., Xiong, H., Zhang, F. & Kim, J. S. (2023). *Coord. Chem. Rev.* **476**, 214908.
Martínez-Bourget, D., Rocha, E., Labra-Vázquez, P., Santillan, R., Ortiz-López, B., Ortiz-Navarrete, V., Maraval, V., Chauvin, R. & Farfán, N. (2022). *Spectrochim. Acta A Mol. Biomol. Spectrosc.* **283**, 121704.
Ordóñez-Hernández, J., Arcos-Ramos, R., Alvarez-Venicio, V., Basiuk, V. A., González-Antonio, O., Flores-Álamo, M., García-Ortega, H., Farfán, N. & Carreón-Castro, M. P. (2021). *J. Mol. Struct.* **1239**, 130437.
Polianskaia, Z. A., Larionov, A. S., Khrustalev, V. N., Akkurt, M., Manahelohe, G. M., Guliyeva, N. A. & Hasanov, K. I. (2026). *Acta Cryst.* E**82**, 505–510.
Prieto–Montero, R., Prieto–Castañeda, A., Sola–Llano, R., Agarrabeitia, A. R., García–Fresnadillo, D., López–Arbeloa, I., Villanueva, A., Ortiz, M. J., de la Moya, S. & Martínez–Martínez, V. (2020). *Photochem. Photobiol.* **96**, 458–477.
Sadikhova, N. D., Atioğlu, Z., Guliyeva, N. A., Shelukho, E. R., Polyanskaya, D. K., Khrustalev, V. N., Akkurt, M. & Bhattarai, A. (2024). *Acta Cryst.* E**80**, 72–77.
Schmitt, A., Hinkeldey, B., Wild, M. & Jung, G. (2009). *J. Fluoresc.* **19**, 755–758.
Sheldrick, G. M. (2008). *Acta Cryst.* A**64**, 112–122.
Sheldrick, G. M. (2015). *Acta Cryst.* C**71**, 3–8.
Šoltysová, M., Güixens-Gallardo, P., Sieglová, I., Soldánová, A., Krejčiříková, V., Fábry, M. & Řezáčová, P. (2025). RSC *Chem. Biol.* **6**, 376–386.
Spackman, P. R., Turner, M. J., McKinnon, J. J., Wolff, S. K., Grimwood, D. J., Jayatilaka, D. & Spackman, M. A. (2021). *J. Appl. Cryst.* **54**, 1006–1011.
Spek, A. L. (2020). *Acta Cryst.* E**76**, 1–11.
Treibs, A. & Kreuzer, F. H. (1968). *Justus Liebigs Ann. Chem.* **718**, 208–223.
Xochitiotzi-Flores, E., Islas-Mejía, A. A., García-Ortega, H., Romero-Ávila, M., Mendez-Stivalet, J. M., Carreón-Castro, M. P., Santillan, R., Maldonado-Domínguez, M., Arcos-Ramos, R. & Farfán, N. (2016). *J. Organomet. Chem.* **805**, 148–157.
Yadav, I. S. & Misra, R. (2023). *J. Mater. Chem.* C**11**, 8688–8723.
Zhang, W., Ahmed, A., Cong, H., Wang, S., Shen, Y. & Yu, B. (2021). *Dyes Pigments* **185**, 108937.

supporting information

Acta Cryst. (2026). E**82**, 871-876 [https://doi.org/10.1107/S205698902600647X]

Crystal structure and Hirshfeld surface analysis of 10-([2,3′-bithiophen]-5′-yl)-5,5-difluoro-5*H*-4λ^4,5λ^4-dipyrrolo[1,2-*c*:2′,1′-*f*][1,3,2]diazaborinine

Darya K. Polyanskaya, Zlata A. Polianskaia, Victor N. Khrustalev, Mehmet Akkurt, Gizachew Mulugeta Manahelohe, Khudayar I. Hasanov and Narmina A. Guliyeva

Computing details

10-([2,3′-Bithiophen]-5′-yl)-5,5-difluoro-5*H*-4λ^4,5λ^4-dipyrrolo[1,2-*c*:2′,1′-*f*][1,3,2]diazaborinine

Crystal data

$C_{17}H_{11}BF_2N_2S_2$
M_r = 356.21
Monoclinic, $P2_1$
a = 9.4693 (2) Å
b = 7.2412 (1) Å
c = 11.2392 (2) Å
β = 95.512 (1)°
V = 767.10 (2) Å^3
Z = 2
$F(000)$ = 364
D_x = 1.542 Mg m^{-3}
Mo $K\alpha$ radiation, λ = 0.71073 Å
Cell parameters from 9989 reflections
θ = 3.0–32.3°
μ = 0.37 mm^{-1}
T = 100 K
Prism, red
0.20 × 0.12 × 0.10 mm

Data collection

Bruker D8 QUEST PHOTON-III area detector diffractometer
Radiation source: fine-focus sealed X-ray tube
φ and ω scans
Absorption correction: multi-scan (SADABS; Krause *et al.*, 2015)
T_{min} = 0.674, T_{max} = 0.746
24975 measured reflections
5559 independent reflections
5142 reflections with $I > 2\sigma(I)$
R_{int} = 0.041
θ_{max} = 32.6°, θ_{min} = 2.7°
h = −14→14
k = −10→10
l = −17→17

Refinement

Refinement on F^2
Least-squares matrix: full
$R[F^2 > 2\sigma(F^2)]$ = 0.030
$wR(F^2)$ = 0.072
S = 1.03
5559 reflections
255 parameters
147 restraints
Primary atom site location: difference Fourier map
Secondary atom site location: difference Fourier map
Hydrogen site location: inferred from neighbouring sites
H-atom parameters constrained
$w = 1/[\sigma^2(F_o^2) + (0.0365P)^2 + 0.1049P]$ where $P = (F_o^2 + 2F_c^2)/3$
$(\Delta/\sigma)_{max} < 0.001$
$\Delta\rho_{max}$ = 0.35 e Å^{-3}
$\Delta\rho_{min}$ = −0.22 e Å^{-3}
Absolute structure: Refined as an inversion twin
Absolute structure parameter: 0.29 (6)

Special details

Geometry. All esds (except the esd in the dihedral angle between two l.s. planes) are estimated using the full covariance matrix. The cell esds are taken into account individually in the estimation of esds in distances, angles and torsion angles; correlations between esds in cell parameters are only used when they are defined by crystal symmetry. An approximate (isotropic) treatment of cell esds is used for estimating esds involving l.s. planes.

Refinement. Refined as a 2-component inversion twin.

Fractional atomic coordinates and isotropic or equivalent isotropic displacement parameters (Å²)

	x	*y*	*z*	U_{iso}*/U_{eq}	Occ. (<1)
S1	0.33169 (4)	0.33970 (7)	0.83032 (3)	0.01449 (9)	
C14	0.71857 (18)	0.4686 (3)	0.97857 (15)	0.0151 (3)	
S2	0.7570 (2)	0.3378 (3)	1.1014 (2)	0.0156 (3)	0.659 (3)
C15	0.8301 (13)	0.5897 (19)	0.9628 (11)	0.027 (2)	0.659 (3)
H15	0.828588	0.673475	0.897655	0.032*	0.659 (3)
C16	0.9441 (13)	0.5772 (19)	1.0512 (11)	0.0196 (13)	0.659 (3)
H16	1.027020	0.651489	1.054491	0.024*	0.659 (3)
C17	0.9198 (11)	0.445 (2)	1.1313 (11)	0.0156 (14)	0.659 (3)
H17	0.985589	0.413450	1.197436	0.019*	0.659 (3)
S2′	0.8456 (6)	0.6140 (8)	0.9467 (5)	0.0186 (7)	0.341 (3)
C15′	0.768 (2)	0.368 (3)	1.0892 (19)	0.021 (3)	0.341 (3)
H15A	0.714098	0.273369	1.121888	0.026*	0.341 (3)
C16′	0.899 (2)	0.425 (4)	1.141 (2)	0.017 (3)	0.341 (3)
H16A	0.944480	0.381311	1.215129	0.020*	0.341 (3)
C17′	0.953 (3)	0.551 (4)	1.071 (2)	0.022 (3)	0.341 (3)
H17A	1.044587	0.602867	1.088825	0.027*	0.341 (3)
F1	0.21820 (11)	0.35646 (18)	0.28958 (9)	0.0187 (2)	
F2	0.23232 (12)	0.66759 (18)	0.26818 (11)	0.0211 (2)	
N1	0.41373 (15)	0.5112 (2)	0.39744 (12)	0.0127 (3)	
N2	0.17288 (15)	0.5490 (2)	0.45742 (13)	0.0138 (3)	
C1	0.52374 (18)	0.4979 (3)	0.33101 (16)	0.0154 (3)	
H1	0.517554	0.510899	0.246561	0.018*	
C2	0.64899 (19)	0.4620 (3)	0.40412 (16)	0.0154 (3)	
H2	0.741425	0.449050	0.378963	0.019*	
C3	0.61206 (17)	0.4491 (3)	0.52039 (16)	0.0138 (3)	
H3	0.674394	0.423098	0.589710	0.017*	
C4	0.46383 (17)	0.4819 (2)	0.51653 (15)	0.0122 (3)	
C5	0.37090 (17)	0.4875 (2)	0.60681 (15)	0.0119 (3)	
C6	0.22474 (18)	0.5219 (2)	0.57619 (15)	0.0131 (3)	
C7	0.11248 (18)	0.5563 (3)	0.64747 (16)	0.0157 (3)	
H7	0.117053	0.548041	0.732113	0.019*	
C8	−0.00633 (19)	0.6045 (3)	0.57061 (18)	0.0184 (4)	
H8	−0.097830	0.634997	0.592717	0.022*	
C9	0.03554 (19)	0.5994 (3)	0.45480 (18)	0.0178 (4)	
H9	−0.024200	0.627299	0.384311	0.021*	
C10	0.42658 (17)	0.4603 (2)	0.73114 (15)	0.0125 (3)	
C11	0.55834 (17)	0.5100 (2)	0.78462 (15)	0.0128 (3)	
H11	0.624807	0.580531	0.745589	0.015*	

C12	0.58456 (18)	0.4450 (2)	0.90406 (15)	0.0135 (3)
C13	0.46880 (17)	0.3523 (3)	0.93995 (14)	0.0154 (3)
H13	0.465755	0.301006	1.017451	0.018*
B1	0.2566 (2)	0.5224 (3)	0.34767 (17)	0.0146 (3)

Atomic displacement parameters (Å²)

	U^{11}	U^{22}	U^{33}	U^{12}	U^{13}	U^{23}
S1	0.01389 (16)	0.01582 (17)	0.01392 (16)	−0.00373 (16)	0.00209 (13)	0.00032 (17)
C14	0.0145 (7)	0.0175 (8)	0.0128 (7)	0.0011 (6)	0.0000 (6)	−0.0020 (6)
S2	0.0171 (5)	0.0170 (8)	0.0122 (5)	0.0015 (5)	−0.0016 (4)	0.0033 (4)
C15	0.038 (4)	0.024 (4)	0.018 (3)	0.004 (3)	−0.001 (2)	0.006 (2)
C16	0.020 (3)	0.022 (3)	0.018 (3)	−0.002 (2)	0.005 (2)	0.004 (2)
C17	0.012 (3)	0.022 (4)	0.012 (3)	0.0026 (19)	−0.002 (2)	0.001 (2)
S2′	0.0174 (9)	0.0240 (15)	0.0129 (13)	−0.0027 (8)	−0.0057 (9)	0.0055 (10)
C15′	0.023 (4)	0.021 (7)	0.021 (6)	−0.006 (4)	0.009 (3)	0.002 (4)
C16′	0.020 (6)	0.018 (5)	0.012 (4)	0.001 (4)	0.006 (4)	0.006 (3)
C17′	0.018 (4)	0.028 (8)	0.019 (7)	0.000 (4)	−0.005 (4)	0.004 (4)
F1	0.0164 (4)	0.0208 (5)	0.0188 (5)	−0.0043 (5)	0.0012 (4)	−0.0067 (5)
F2	0.0189 (5)	0.0240 (6)	0.0193 (5)	−0.0007 (4)	−0.0029 (4)	0.0068 (4)
N1	0.0118 (6)	0.0140 (6)	0.0121 (6)	−0.0017 (5)	0.0010 (5)	0.0003 (5)
N2	0.0108 (6)	0.0146 (6)	0.0156 (6)	0.0000 (5)	−0.0008 (5)	−0.0015 (5)
C1	0.0151 (7)	0.0169 (8)	0.0143 (7)	−0.0023 (6)	0.0026 (6)	−0.0005 (6)
C2	0.0132 (7)	0.0167 (8)	0.0168 (7)	−0.0007 (6)	0.0040 (6)	−0.0003 (6)
C3	0.0116 (7)	0.0137 (7)	0.0161 (7)	0.0001 (6)	0.0010 (6)	0.0006 (6)
C4	0.0109 (6)	0.0134 (7)	0.0121 (7)	−0.0005 (6)	0.0006 (5)	0.0003 (6)
C5	0.0116 (6)	0.0102 (7)	0.0135 (7)	−0.0010 (5)	−0.0004 (5)	−0.0013 (5)
C6	0.0112 (6)	0.0137 (7)	0.0143 (7)	−0.0005 (6)	0.0011 (5)	−0.0027 (6)
C7	0.0128 (7)	0.0166 (8)	0.0178 (7)	−0.0012 (6)	0.0023 (6)	−0.0043 (6)
C8	0.0113 (7)	0.0191 (8)	0.0246 (9)	0.0011 (6)	0.0016 (7)	−0.0057 (7)
C9	0.0116 (7)	0.0180 (8)	0.0231 (9)	0.0013 (6)	−0.0025 (7)	−0.0028 (7)
C10	0.0132 (7)	0.0122 (7)	0.0124 (7)	−0.0013 (6)	0.0026 (5)	0.0001 (6)
C11	0.0126 (7)	0.0129 (7)	0.0130 (7)	−0.0010 (6)	0.0018 (5)	−0.0006 (6)
C12	0.0138 (7)	0.0145 (7)	0.0122 (7)	−0.0007 (6)	0.0011 (6)	−0.0007 (6)
C13	0.0164 (7)	0.0165 (7)	0.0133 (6)	−0.0017 (7)	0.0010 (5)	−0.0001 (7)
B1	0.0134 (8)	0.0158 (8)	0.0142 (8)	−0.0018 (7)	−0.0008 (6)	−0.0006 (7)

Geometric parameters (Å, º)

S1—C13	1.7043 (17)	N2—C9	1.348 (2)
S1—C10	1.7334 (17)	N2—C6	1.391 (2)
C14—C15	1.397 (10)	N2—B1	1.541 (2)
C14—C12	1.462 (2)	C1—C2	1.401 (2)
C14—C15′	1.476 (18)	C1—H1	0.9500
C14—S2′	1.664 (5)	C2—C3	1.388 (2)
C14—S2	1.685 (3)	C2—H2	0.9500
S2—C17	1.729 (9)	C3—C4	1.420 (2)
C15—C16	1.398 (15)	C3—H3	0.9500

C15—H15	0.9500	C4—C5	1.406 (2)
C16—C17	1.350 (9)	C5—C6	1.416 (2)
C16—H16	0.9500	C5—C10	1.459 (2)
C17—H17	0.9500	C6—C7	1.413 (2)
S2′—C17′	1.705 (18)	C7—C8	1.395 (3)
C15′—C16′	1.39 (2)	C7—H7	0.9500
C15′—H15A	0.9500	C8—C9	1.397 (3)
C16′—C17′	1.341 (17)	C8—H8	0.9500
C16′—H16A	0.9500	C9—H9	0.9500
C17′—H17A	0.9500	C10—C11	1.380 (2)
F1—B1	1.399 (2)	C11—C12	1.422 (2)
F2—B1	1.385 (2)	C11—H11	0.9500
N1—C1	1.342 (2)	C12—C13	1.378 (2)
N1—C4	1.393 (2)	C13—H13	0.9500
N1—B1	1.541 (2)		

C13—S1—C10	91.83 (8)	C2—C3—C4	107.31 (15)
C15—C14—C12	128.8 (5)	C2—C3—H3	126.3
C12—C14—C15′	127.7 (7)	C4—C3—H3	126.3
C12—C14—S2′	123.8 (2)	N1—C4—C5	120.68 (14)
C15′—C14—S2′	108.4 (7)	N1—C4—C3	107.41 (14)
C15—C14—S2	110.5 (5)	C5—C4—C3	131.91 (15)
C12—C14—S2	120.73 (15)	C4—C5—C6	119.64 (15)
C14—S2—C17	91.5 (4)	C4—C5—C10	119.58 (14)
C14—C15—C16	114.2 (9)	C6—C5—C10	120.77 (15)
C14—C15—H15	122.9	N2—C6—C7	107.68 (15)
C16—C15—H15	122.9	N2—C6—C5	120.32 (15)
C17—C16—C15	110.6 (11)	C7—C6—C5	131.62 (16)
C17—C16—H16	124.7	C8—C7—C6	107.38 (16)
C15—C16—H16	124.7	C8—C7—H7	126.3
C16—C17—S2	113.2 (9)	C6—C7—H7	126.3
C16—C17—H17	123.4	C7—C8—C9	106.62 (16)
S2—C17—H17	123.4	C7—C8—H8	126.7
C14—S2′—C17′	92.4 (8)	C9—C8—H8	126.7
C16′—C15′—C14	114.1 (15)	N2—C9—C8	110.27 (17)
C16′—C15′—H15A	122.9	N2—C9—H9	124.9
C14—C15′—H15A	122.9	C8—C9—H9	124.9
C17′—C16′—C15′	109 (2)	C11—C10—C5	127.63 (15)
C17′—C16′—H16A	125.5	C11—C10—S1	110.75 (13)
C15′—C16′—H16A	125.5	C5—C10—S1	121.47 (12)
C16′—C17′—S2′	116 (2)	C10—C11—C12	113.17 (15)
C16′—C17′—H17A	122.1	C10—C11—H11	123.4
S2′—C17′—H17A	122.1	C12—C11—H11	123.4
C1—N1—C4	108.23 (14)	C13—C12—C11	111.46 (15)
C1—N1—B1	125.17 (14)	C13—C12—C14	124.08 (16)
C4—N1—B1	125.80 (14)	C11—C12—C14	124.43 (16)
C9—N2—C6	108.06 (15)	C12—C13—S1	112.74 (13)
C9—N2—B1	125.85 (15)	C12—C13—H13	123.6

C6—N2—B1	126.08 (14)	S1—C13—H13	123.6
N1—C1—C2	110.22 (15)	F2—B1—F1	109.36 (15)
N1—C1—H1	124.9	F2—B1—N1	111.66 (15)
C2—C1—H1	124.9	F1—B1—N1	108.84 (15)
C3—C2—C1	106.81 (15)	F2—B1—N2	110.79 (15)
C3—C2—H2	126.6	F1—B1—N2	110.52 (15)
C1—C2—H2	126.6	N1—B1—N2	105.61 (14)

C15—C14—S2—C17	0.2 (9)	C6—C7—C8—C9	−0.2 (2)
C12—C14—S2—C17	179.4 (6)	C6—N2—C9—C8	−0.6 (2)
C12—C14—C15—C16	180.0 (9)	B1—N2—C9—C8	178.19 (17)
S2—C14—C15—C16	−0.9 (14)	C7—C8—C9—N2	0.5 (2)
C14—C15—C16—C17	1.4 (19)	C4—C5—C10—C11	32.3 (3)
C15—C16—C17—S2	−1.2 (18)	C6—C5—C10—C11	−146.84 (18)
C14—S2—C17—C16	0.6 (13)	C4—C5—C10—S1	−142.80 (14)
C12—C14—S2′—C17′	−179.3 (12)	C6—C5—C10—S1	38.0 (2)
C15′—C14—S2′—C17′	−1.2 (17)	C13—S1—C10—C11	−1.23 (14)
C12—C14—C15′—C16′	−178.6 (19)	C13—S1—C10—C5	174.63 (15)
S2′—C14—C15′—C16′	3 (3)	C5—C10—C11—C12	−173.38 (17)
C14—C15′—C16′—C17′	−4 (4)	S1—C10—C11—C12	2.2 (2)
C15′—C16′—C17′—S2′	3 (4)	C10—C11—C12—C13	−2.2 (2)
C14—S2′—C17′—C16′	−1 (3)	C10—C11—C12—C14	176.20 (16)
C4—N1—C1—C2	−0.7 (2)	C15—C14—C12—C13	−165.1 (8)
B1—N1—C1—C2	−170.93 (16)	C15′—C14—C12—C13	15.0 (14)
N1—C1—C2—C3	1.3 (2)	S2′—C14—C12—C13	−167.3 (3)
C1—C2—C3—C4	−1.4 (2)	S2—C14—C12—C13	16.0 (3)
C1—N1—C4—C5	−179.88 (16)	C15—C14—C12—C11	16.7 (8)
B1—N1—C4—C5	−9.8 (3)	C15′—C14—C12—C11	−163.2 (14)
C1—N1—C4—C3	−0.1 (2)	S2′—C14—C12—C11	14.5 (4)
B1—N1—C4—C3	169.99 (16)	S2—C14—C12—C11	−162.26 (19)
C2—C3—C4—N1	0.9 (2)	C11—C12—C13—S1	1.2 (2)
C2—C3—C4—C5	−179.35 (18)	C14—C12—C13—S1	−177.18 (14)
N1—C4—C5—C6	0.4 (2)	C10—S1—C13—C12	−0.02 (16)
C3—C4—C5—C6	−179.24 (18)	C1—N1—B1—F2	−55.8 (2)
N1—C4—C5—C10	−178.71 (15)	C4—N1—B1—F2	135.73 (17)
C3—C4—C5—C10	1.6 (3)	C1—N1—B1—F1	65.0 (2)
C9—N2—C6—C7	0.5 (2)	C4—N1—B1—F1	−103.45 (19)
B1—N2—C6—C7	−178.32 (16)	C1—N1—B1—N2	−176.27 (16)
C9—N2—C6—C5	−173.11 (16)	C4—N1—B1—N2	15.2 (2)
B1—N2—C6—C5	8.1 (3)	C9—N2—B1—F2	45.9 (2)
C4—C5—C6—N2	0.4 (2)	C6—N2—B1—F2	−135.48 (17)
C10—C5—C6—N2	179.52 (16)	C9—N2—B1—F1	−75.5 (2)
C4—C5—C6—C7	−171.47 (19)	C6—N2—B1—F1	103.14 (19)
C10—C5—C6—C7	7.7 (3)	C9—N2—B1—N1	166.97 (17)
N2—C6—C7—C8	−0.2 (2)	C6—N2—B1—N1	−14.4 (2)
C5—C6—C7—C8	172.44 (19)		

Hydrogen-bond geometry (Å, º)

D—H···*A*	*D*—H	H···*A*	*D*···*A*	*D*—H···*A*
C3—H3···F2^{i}	0.95	2.55	3.362 (2)	144
C7—H7···S1	0.95	2.68	3.1895 (19)	114
C8—H8···F1^{ii}	0.95	2.43	3.229 (2)	142
C11—H11···F1^{iii}	0.95	2.54	3.4360 (19)	156
C15—H15···F1^{iii}	0.95	2.49	3.426 (13)	168
C17—H17···F1^{iv}	0.95	2.38	3.255 (11)	153

Symmetry codes: (i) −*x*+1, *y*−1/2, −*z*+1; (ii) −*x*, *y*+1/2, −*z*+1; (iii) −*x*+1, *y*+1/2, −*z*+1; (iv) *x*+1, *y*, *z*+1.